THE JOURNAL OF PHYSICAL CHEMISTRY C
A JOURNAL OF THE AMERICAN CHEMICAL SOCIETY

pubs.acs.org/JPCC

Article

Substrate Effects in the Self-Assembling of *N,N*-Diphenylquinodimethyl Thioamide on Transition Metals

Published as part of The Journal of Physical Chemistry virtual special issue "Early-Career and Emerging Researchers in Physical Chemistry Volume 2".

Kai Wang,[‖] Dairong Liu,[‖] Manoj K. Manna, Guang Yang, Linfei Li, Xu Zhang, A. Jean-Luc Ayitou,* and Nan Jiang*

Cite This: https://doi.org/10.1021/acs.jpcc.3c01663

Read Online

ACCESS | Metrics & More | Article Recommendations | Supporting Information

ABSTRACT: Quinoidal acene-thioamides are a new class of organic light-harvesting chromophores used for several applications, including triplet photosensitization and photometric sensing of metal ions. These chromophores' versatility and attractive photophysics make them suitable for engineering transition-metal−organic hybrid photomaterials. In this regard, we investigated the self-assembly and behavior of *N,N*-diphenylquinodimethyl thioamide (Ph_2QDM) nanostructures on transition-metal surfaces for potential applications in photocatalysis and photosensors. In this work, Ph_2QDM molecules were deposited onto Au(111), Au(100), and Ag(100) surfaces. The scanning tunneling microscopy (STM) images indicate that the Ph_2QDM molecules form an amorphous structure on Au(111) but self-assembled structures on Au(100) and Ag(100). Furthermore, the isolated single sulfur atoms are found on Ag(100) but not on Au substrates. High-resolution STM images combined with density functional theory (DFT) simulation results indicate that the Ph_2QDM molecules experience desulfurization on Ag(100) that induces the cleaving of the C═S bond and new covalent bonds between the desulfurized Ph_2QDM and Ag atoms. The present results not only uncover the effect of substrates on the self-assembly of Ph_2QDM but also open new avenues for metal−organic catalysts and nanodevices.

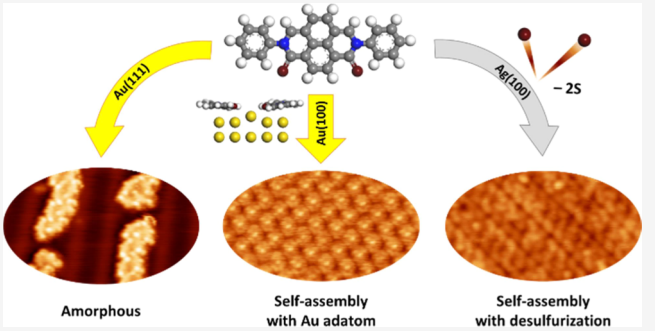

INTRODUCTION

Thioamides belong to the broader class of carbonyl compounds with a carbon−sulfur double bond (C═S), with much smaller bond dissociation energies than a typical carbon−oxygen bond energy.[1,2] However, incorporating sulfur into several carbonyl derivatives has been employed to fine-tune the optoelectronic and/or chemophysical properties of the corresponding thio-containing systems,[3−5] including improved internal charge mobility in thioamide molecules vs in classical amides[6,7]−−with more charge transfer from nitrogen to thiocarbonyl bond than from nitrogen to carbonyl bond in the corresponding amides.[8−10] This establishes that thioamide molecules exhibit higher reactivity and attractive optoelectronic properties than classical amides.[11−13] Hence, exploring thioamide-containing compounds will open new avenues to tailor these scaffolds for novel heterocyclic chemistry,[14−17] pharmaceuticals,[18−22] agrochemicals,[23,24] and photochemical sensitization.[25−27]

In recent years, increasing attention has been received on thioamide transition-metal complexes due to their high catalytic activities and the nature of the C═S bond.[28−31] So far, thioamide transition-metal complex catalysts have been extensively employed in the Mizorroki−Heck reaction,[32,33] Suzuki−Miyaura reaction,[32,34] amide synthesis,[35] alcohol oxidation,[36] and C−H bond functionalization.[37−43] The remarkable catalytic performance of thioamide transition-metal complexes inspires people to investigate the interaction of thioamides with transition metals, especially thioamide self-assembly on transition-metal surfaces that hold promise as a novel catalytic system.[44−46] In this regard, various simple thioamide molecules, such as thiadiazole,[44] 2-mercapto pyrimidine,[47,48] and thiourea[49,50] deposited on metal surfaces, have been studied. Despite their better stability and catalytic reactivity, the on-surface self-assembly of novel exotic thioamide molecules remain largely unexplored.[51,52]

N,N-Diphenylquinodimethyl thioamide (Ph_2QDM) belongs to a new class of quinoidal acene-thioamides with a C_2 (or C_{2v})

Received: March 11, 2023
Revised: July 2, 2023

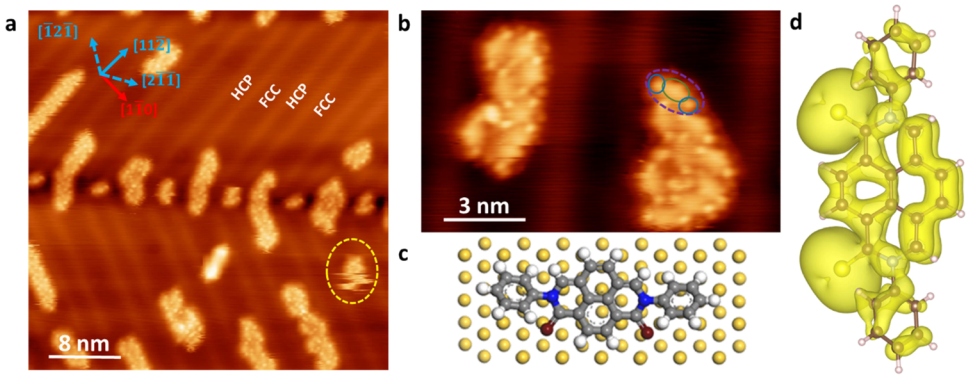

Figure 1. (a) Large-scale STM image of Ph_2QDM molecules on Au(111). (b) Zoomed-in image with single Ph_2QDM molecules resolved. A Ph_2QDM molecule is indicated by a dashed-line oval, and its naphthalene-like ring and benzene rings are marked by the green oval and blue circles, respectively. The bias voltage is 0.5 V for panel (a) and −1 V for panel (b); I_{set} = 100 pA for both images. (c) Simulated model for a Ph_2QDM molecule on the Au(111) substrate. (d) The simulated density distribution for states between E_f −1 eV and E_f, E_f is the Fermi energy.

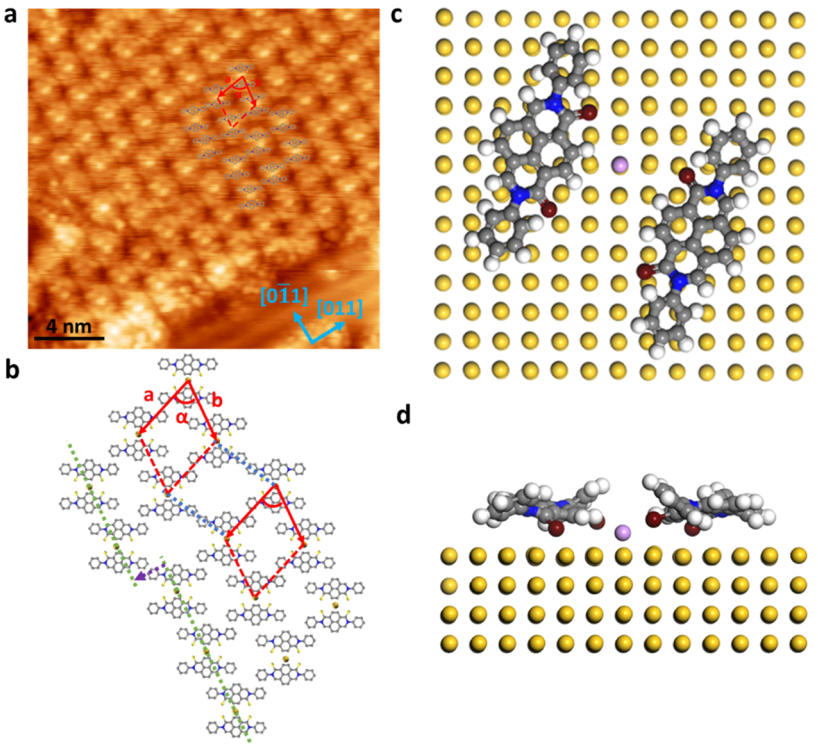

Figure 2. (a) Self-assembly island of Ph_2QDM on Au(100), V_{bias} = −0.02 V, I_{set} = 100 pA. The lattice constant is measured to be around a = 1.84 ± 0.04, b = 1.88 ± 0.04 nm, α = 70 ± 2°, (b) molecular self-assembly model derived from panel (a). Top view (c) and side view (d) of the simulated model for a Au atom (purple) sandwiched by two Ph_2QDM molecules.

symmetric scaffold.[53−55] Ph_2QDM contains a cyclo-thioamide moiety and a fused proaromatic quinoidal ring to a Clar sextet. We reported earlier that the proaromatic characteristic of all other reported quinoidal acene-thioamides is the major factor influencing these chromophores' optoelectronic and photo-excited-state behavior.[55] These unique characteristics of the quinoidal acene-thioamide chromophores have been extensively exploited/harnessed for several processes, such as the triplet photosensitization[56−59] and photometric sensing of heavy metal ions.[60] To further explore the behavior of quinoidal acene-thioamide chromophores on metal surfaces, we investigated the adsorption and self-assembly of Ph_2QDM on atomic well-defined metal surfaces, specifically Au(111), Au(100), and Ag(100) single-crystal surfaces using scanning tunneling microscopy (STM). In contrast to the amorphous structures on Au(111), Ph_2QDM molecules formed self-assembled structures on Au(100) and Ag(100). Importantly, desulfurization from the Ph_2QDM/Ag(100) samples was observed, whereas samples of Ph_2QDM/Au(111) or Ph_2QDM/Au(100) underwent classical morphological changes depending on the crystallinity of the substrate. These distinctly different adsorptive behaviors of Ph_2QDM suggest a strong substrate effect, which will inform the investigation of the surface chemistry of quinoidal acene-thioamide chromophore self-assembly on transition metals.

METHODS

Sample Preparation and STM Study. Experiments were carried out in a variable-temperature STM system (UNISOKU, USM1400) under a base pressure of 10^{-10} Torr. The

https://doi.org/10.1021/acs.jpcc.3c01663
J. Phys. Chem. C XXXX, XXX, XXX−XXX

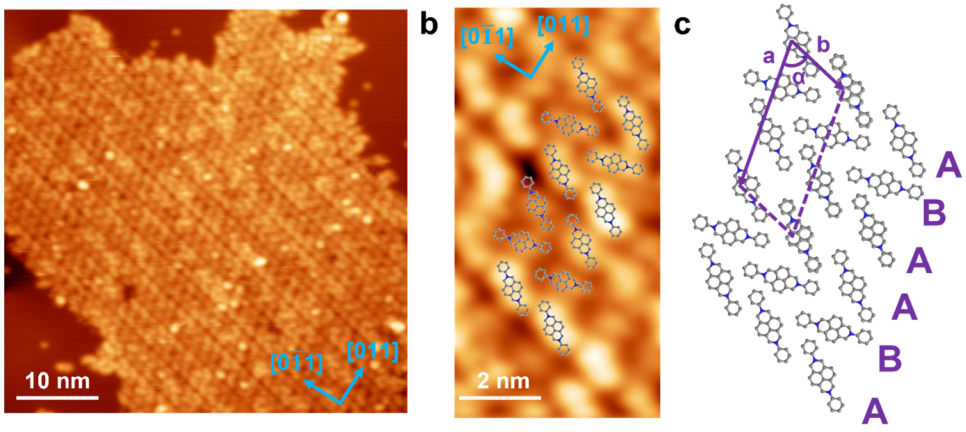

Figure 3. (a) STM image of a self-assembly island of Ph_2QDM on Ag(100). (b) Zoomed-in STM image with molecular models superimposed. The lattice constant is measured to be about a = 3.11 ± 0.12 nm b = 1.43 ± 0.08 nm, and α = 68 ± 2°. (c) The arrangement of the self-assembled structure derived from panel (b). The bias voltage is −0.5 V for (a) and 0.3 V for (b); I_{set} = 100 pA for both images.

sample was prepared in a chamber (with base pressure 2.2 × 10^{-10} Torr) separated from the STM chamber by a gate valve. The Au(111), Au(100), and Ag(100) surfaces were cleaned via repeated cycles of argon ion sputtering (1 kV, ∼9.0 × 10^{-6} Torr) and thermal annealing to 865 K. The synthesis and characterization of Ph_2QDM are described in the Supporting Information (Scheme S1 and Figures S3 and S4). The molecules were sublimed onto the clean metal surfaces via a K-cell molecular evaporator (TCE-BSC, Kentax GmbH) for 4 min (220 °C), while the substrates were kept at room temperature during deposition. After that, the samples were transferred to the analysis chamber for STM characterizations performed at a liquid nitrogen temperature (78 K). Electrochemically etched Ag tips were used for STM experiments,[61] and the STM images were analyzed using the WSxM[62] program provided by Nanotech.

Computational Parameters. The VASP package[63] was employed to perform density functional theory (DFT) calculations with the projector augmented wave pseudopotentials[64] and the Perdew−Burke−Ernzerhof generalized gradient approximation.[65] The van der Waals (vdW) interaction was included by using a nonlocal correlation functional.[66,67] An energy cutoff of 400 eV was used for the plane-wave basis set. Only the Γ-point in the Brillouin zone was used considering the large size of the supercell. We employed a four-layer slab with a (5 × 5) unit cell for the Ag(100) and Au(100) surfaces. A four-layer slab with an (8 × 4) unit cell is exploited to model the Au(111) surface. The atoms in the top two layers were fully relaxed, while the rest of the atoms were fixed in their equilibrium positions. The force convergence criterion for atomic relaxation is 0.01 eV/Å.

RESULTS AND DISCUSSION

Given the particular interaction between sulfur and gold that facilitates molecular self-assembly on Au surfaces,[68−71] we first studied the adsorption of Ph_2QDM on Au(111). As shown in Figure 1a, the molecules form small islands along the herringbone reconstruction of Au(111).[72] The structure of a single Ph_2QDM molecule can be resolved as one oval protrusion (marked by the green oval) with two round dots (marked by two blue circles), shown in Figure 2b. The oval protrusion is identified as a naphthalene-like ring, while the two bright dots are assigned to benzene rings (the *N*-phenyl) on both sides. Notably, the shape of the molecular framework is slightly bent, resulting from the C_{2v} symmetry/point group, which agrees with the simulated model shown in Figures 1c and S7. There are two possible reasons why the molecules cannot form larger islands. First, based on the previous reports, the Au(111) herringbone divides the surface into the face-centered-cubic (FCC) and hexagonal-close-pack (HCP) sites (marked in Figure 1a), which have different affinities to molecules.[72−76] For the Ph_2QDM, most islands are located on the FCC site surface, where the elbow sites are more favored. Very few of the molecules were observed on the HCP site surface and only at the elbows (Figure 1a). Similar preferential nucleation phenomena at the elbow sites have been reported for various metals and molecules.[72,75−79] However, the growth across the herringbone reconstruction is forbidden, prohibiting the formation of large molecular islands. Another reason involves molecular orientations. Figure 1b shows that the arrangement of Ph_2QDM molecules is irregular with random orientations (see the angle distribution in Figure S5), which could also prevent the islands from forming order self-assembly and growing bigger. Meanwhile, it is notable that in Figure 1a, a diffusive molecular island was observed (yellow dashed circle), which demonstrates the weak interaction between Ph_2QDM molecules. Furthermore, neither annealing the sample to a high temperature (175 °C) nor increasing the molecular coverage (0.6 ML) can result in self-assembled patterns (Figure S6). Consequently, only disordered molecular islands are present on Au(111).

Since the reconstruction of Au(111) impedes the formation of the Ph_2QDM self-assembly, it is worthwhile to study the adsorption of this chromophore on another Au substrate. With a fourfold symmetry and narrower reconstruction structures, Au(100) surfaces have been reported to host different self-assemblies from Au(111) surfaces.[80,81] As shown in Figure 2, Ph_2QDM molecules form a self-assembly spot-like pattern, where a bright protrusion is present in each molecular pairs. The protrusion is assigned to a Au adatom grabbed from the surface reconstruction structure by the neighboring S atoms, which indicates a strong interaction between molecules and the substrate. In addition, we observed that there is a sliding of the self-assembly structure seen in Figure 2a, highlighted by the two identical red lattice and blue dashed lines in Figure 2b; the purple arrow and two dashed green lines indicate the direction of sliding, and the distance of sliding is measured to be about 0.68 nm. Moreover, from the lower right part of the image, the

https://doi.org/10.1021/acs.jpcc.3c01663
J. Phys. Chem. C XXXX, XXX, XXX−XXX

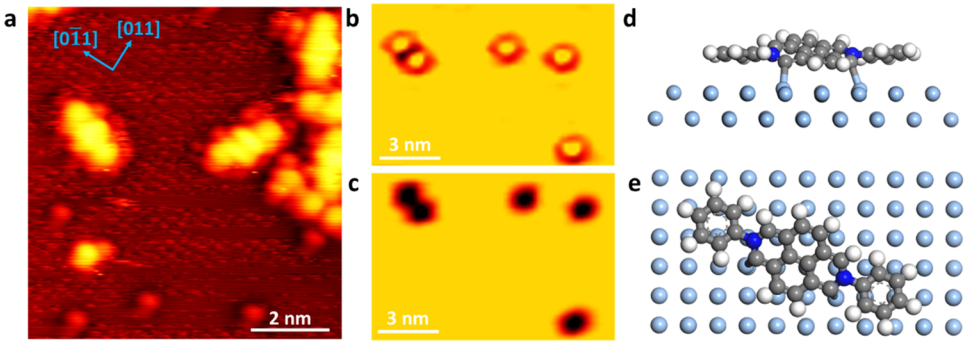

Figure 4. (a) STM image of single Ph_2QDM molecules and isolated sulfur atoms on the Ag(100) surface. (b, c) Sulfur atoms imaged at different biases. The bias voltage is −2 V for panels (a) and (b) but 2 V for (c). I_{set} = 100 pA for all three images. (d, e) Simulated model of a desulfurized Ph_2QDM molecule on the Ag(100) substrate in the side view (d) and plain view (e).

reconstruction of Au(100) can be seen. Different from the random orientation on Au(111), the molecules on Au(100) are found to have a constant angle of about 21 ± 2° with respect to the [011] direction,[82−86] which matches with the simulated model (Figure 2c,d). The consistent orientation observed on Au(100) suggests a stronger interaction between the surface and the molecules, facilitating the self-assembly of Ph_2QDM on Au(100).

The different absorption behaviors on Au(111) and Au(100) indicate the effect of substrate symmetry on the Ph_2QDM molecular self-assembly. In addition to lattice structures, the chemistry of substrates plays a key role in molecular adsorption and self-assembly. To gain insights in this regard, a Ag(100) substrate, which shares the same lattice symmetry with Au(100) was used to probe the surface behavior of Ph_2QDM. As a result, a different self-assembly island with a stripe-like structure was obtained (Figure 3a). The STM image in Figure 3b indicates that the stripe consists of a periodic arrangement of Ph_2QDM molecules in an "ABA" structure (Figure 3b,c), all of the molecules are in a straight rodlike configuration with a length of 1.6 nm, which agrees with the configuration of isolated molecules and the simulated model (Figure 4). The molecules in A and B stripes are oriented to 55 ± 4 and 105 ± 3° with respect to the [011] direction of the Ag(100) substrate, respectively.

Distinct from the images obtained on Au(111) and Au(100) substrates, we noticed many isolated protrusions near the island on Ag(100) (right top and left bottom of Figure 3a). Figures 4a and S8 show the STM images of the coexisting single Ph_2QDM molecules and randomly distributed protrusions on Ag(100). Remarkably, the protrusions surrounded with dark rings change to depressions when the scanning bias is switched from −2 to 2 V, as displayed in Figure 4b,c. The bias-dependent topography and the apparent size of the protrusions (∼1.5 nm) are in agreement with the reported characteristics of sulfur atoms.[87−89] Significantly, the shape of Ph_2QDM molecules appear to be straight, in contrast to the curved molecular shape observed on Au(111) and Au(100). This observation conforms to the unique structural features of Ph_2QDM, suggesting the desulfurization of Ph_2QDM molecules on Ag(100).

Since the purity of Ph_2QDM has been confirmed (Supporting Information 1, Figures S3 and S4), the existence of isolated single sulfur atoms on the surface indicates plausible desulfurization of Ph_2QDM/Ag(100), leaving behind a quasi-aromatized scaffold. To further confirm this conjecture, the model of the sulfur-cleaved Ph_2QDM adsorbed on the Ag(100) surface is simulated; as shown in Figure 4d,e, the two unsaturated carbon atoms due to the desulfurization form bonds with two Ag atoms, respectively, and drag them slightly out of the surface, with a bond length of around 2.3 Å. Furthermore, based on the analysis of the atomic resolution of Ag(100) shown in Figure 4a, the isolated Ph_2QDM molecules were found to be oriented to an angle of 25.8° with respect to the [0$\bar{1}$1] or [011] directions. This value agrees very well with the angle (∼24°) measured in the simulated model (Figure 4e). The orientations of the isolated molecules are different from those in the self-assembly structure (55 and 105°), indicating strong intermolecular interactions in the self-assembly structure, which alter the molecular orientation when the self-assembly is formed. It is notable that the sulfur atoms are only observed on the Ag(100) surface rather than Au(100) or Au(111), indicating that compared to Au surfaces, Ag surfaces are more catalytically active during the desulfurization of Ph_2QDM molecules. A similar C═S cleavage process in a redox reaction via the catalysis of silver ions has been observed under the solution phase,[90−92] but the findings from our surface science studies are unprecedented and could open new avenues to explore metal-catalyzed desulfurization of sulfur-containing molecules.

CONCLUSIONS

In summary, we investigated the adsorption and self-assembly of Ph_2QDM on Au(111), Au(100), and Ag(100) surfaces using STM. The STM images show that Ph_2QDM molecules form amorphous islands on Au(111) but orderly self-assembled structures on Au(100) and Ag(100). While most Ph_2QDM molecules prefer to form paired structures on Au(100), inserting coordinated substrate Au atoms resulted in bright protrusions in the self-assembled structure. In addition, an "ABA" arrangement of molecular self-assembly can be observed on Ag(100). Importantly, isolated sulfur atoms are found in Ph_2QDM-deposited Ag(100) surfaces, indicating the Ag-assisted activation of carbon−sulfur double bonds. Consequently, our study uncovers the substrate-dependent self-assembly behavior of Ph_2QDM, which would inform the ongoing effort to realize Ph_2QDM-based nanodevice applications in catalysis, optoelectronics, and photosensing.

https://doi.org/10.1021/acs.jpcc.3c01663
J. Phys. Chem. C XXXX, XXX, XXX−XXX

■ ASSOCIATED CONTENT

Supporting Information

The Supporting Information is available free of charge at https://pubs.acs.org/doi/10.1021/acs.jpcc.3c01663.

Synthesis and characterization of Ph_2QDM; angle distribution of Ph_2QDM molecules on the Au(111) surface; Ph_2QDM molecules on Au(111) at high coverage and after annealing to 175 °C; computational result of Ph_2QDM molecules on Au(111); large-scale image of Ph_2QDM on Ag(100); and plausible charge redistribution of Ph_2QDM (PDF)

■ AUTHOR INFORMATION

Corresponding Authors

Nan Jiang − *Department of Chemistry, University of Illinois Chicago, Chicago, Illinois 60607, United States;* orcid.org/0000-0002-4570-180X; Email: njiang@uic.edu

A. Jean-Luc Ayitou − *Department of Chemistry, University of Illinois Chicago, Chicago, Illinois 60607, United States; Department of Chemistry, Illinois Institute of Technology, Chicago, Illinois 60616, United States;* orcid.org/0000-0001-6355-2564; Email: aayitou@uic.edu

Authors

Kai Wang − *Department of Chemistry, University of Illinois Chicago, Chicago, Illinois 60607, United States*

Dairong Liu − *Department of Chemistry, University of Illinois Chicago, Chicago, Illinois 60607, United States;* orcid.org/0000-0002-9569-8207

Manoj K. Manna − *Department of Chemistry, Illinois Institute of Technology, Chicago, Illinois 60616, United States;* orcid.org/0000-0003-1469-6494

Guang Yang − *Department of Chemistry, University of Illinois Chicago, Chicago, Illinois 60607, United States*

Linfei Li − *Department of Chemistry, University of Illinois Chicago, Chicago, Illinois 60607, United States;* orcid.org/0000-0002-5217-3005

Xu Zhang − *Department of Physics and Astronomy, California State University Northridge, Northridge, California 91330, United States;* orcid.org/0000-0002-6491-3234

Complete contact information is available at: https://pubs.acs.org/10.1021/acs.jpcc.3c01663

Author Contributions

‖K.W. and D.L. contributed equally to this work.

Notes

The authors declare no competing financial interest.

■ ACKNOWLEDGMENTS

K.W., D.L., and N.J. acknowledge support from the National Science Foundation (CHE-1944796). X.Z. acknowledges support from the National Science Foundation (DMR-1828019). This material was based upon work supported by the National Science Foundation under a CAREER grant no. 2211296 awarded to A.J.-l.A. The authors thank postdoc Dr. Abed Jamhawi for helping with a one-step quick purification of Ph_2QDM.

■ REFERENCES

(1) Murai, T. Synthesis of Thioamides. In *Chemistry of Thioamides*; Murai, T., Ed.; Springer Singapore: Singapore, 2019; pp 45−73.

(2) Braverman, S.; Reisman, D. Sulfur-Oxygen Versus Carbon-Oxygen Bond Fission in the Solvolysis of Benzyl Sulfenates. *Tetrahedron Lett.* **1973**, *14*, 3563−3564.

(3) Zhang, H.; Guo, Y.; Wu, Z.; Wang, Y.; Sun, Y.; Feng, X.; Wang, H.; Zhao, G. Unveiling the Theoretical Mechanism of Purely Organic Room Temperature Phosphorescence Emission and Heteroatomic Effects on Singlet-Triplet Intersystem Crossing for Isopropylthioxanthone Derivatives. *J. Lumin.* **2021**, *232*, No. 117864.

(4) Ashwood, B.; Pollum, M.; Crespo-Hernández, C. E. Photochemical and Photodynamical Properties of Sulfur-Substituted Nucleic Acid Bases. *Photochem. Photobiol.* **2019**, *95*, 33−58.

(5) Pollum, M.; Jockusch, S.; Crespo-Hernández, C. E. 2,4-Dithiothymine as a Potent Uva Chemotherapeutic Agent. *J. Am. Chem. Soc.* **2014**, *136*, 17930−17933.

(6) Begum, R. A.; Powell, D.; Bowman-James, K. Thioamide Pincer Ligands with Charge Versatility. *Inorg. Chem.* **2006**, *45*, 964−966.

(7) Mujika, J. I.; Matxain, J. M.; Eriksson, L. A.; Lopez, X. Resonance Structures of the Amide Bond: The Advantages of Planarity. *Chem. - Eur. J.* **2006**, *12*, 7215−7224.

(8) Nasr-Esfahani, M.; Montazerozohori, M.; Moghadam, M.; Mohammadpoor-Baltork, I.; Moradi, S. A Convenient and Inexpensive Method for Conversion of Thioamide Compounds to Their Oxo Derivatives Using Acidified Iodine Monochloride. *J. Sulphur Chem.* **2009**, *30*, 17−21.

(9) Wiberg, K. B.; Rablen, P. R. Why Does Thioformamide Have a Larger Rotational Barrier Than Formamide? *J. Am. Chem. Soc.* **1995**, *117*, 2201−2209.

(10) Wiberg, K. B.; Rush, D. J. Solvent Effects on the Thioamide Rotational Barrier: An Experimental and Theoretical Study. *J. Am. Chem. Soc.* **2001**, *123*, 2038−2046.

(11) Wipf, P.; Hayes, G. B. Synthesis of Oxazines and Thiazines by Cyclodehydration of Hydroxy Amides and Thioamides. *Tetrahedron* **1998**, *54*, 6987−6998.

(12) Miwa, J. H.; Pallivathucal, L.; Gowda, S.; Lee, K. E. Conformational Stability of Helical Peptides Containing a Thioamide Linkage. *Org. Lett.* **2002**, *4*, 4655−4657.

(13) Goldberg, J. M.; Batjargal, S.; Petersson, E. J. Thioamides as Fluorescence Quenching Probes: Minimalist Chromophores to Monitor Protein Dynamics. *J. Am. Chem. Soc.* **2010**, *132*, 14718−14720.

(14) Jagodziński, T. S. Thioamides as Useful Synthons in the Synthesis of Heterocycles. *Chem. Rev.* **2003**, *103*, 197−228.

(15) Kurpil, B.; Kumru, B.; Heil, T.; Antonietti, M.; Savateev, A. Carbon Nitride Creates Thioamides in High Yields by the Photocatalytic Kindler Reaction. *Green Chem.* **2018**, *20*, 838−842.

(16) Li, S.; Li, L.; Li, Y.; Dai, L.; Liu, C.; Liu, Y.; Li, J.; Lv, J.; Li, P.; Wang, B. Fully Conjugated Donor−Acceptor Covalent Organic Frameworks for Photocatalytic Oxidative Amine Coupling and Thioamide Cyclization. *ACS Catal.* **2020**, *10*, 8717−8726.

(17) Huang, X.; Chen, H.; Huang, Z.; Xu, Y.; Li, F.; Ma, X.; Chen, Y. Visible Light-Induced Difunctionalization of Alkynes: The Synthesis of Thiazoles and 1,1-Dibromo-1-En-3-Ynes. *J. Org. Chem.* **2019**, *84*, 15283−15293.

(18) Dunbar, K. L.; Scharf, D. H.; Litomska, A.; Hertweck, C. Enzymatic Carbon−Sulfur Bond Formation in Natural Product Biosynthesis. *Chem. Rev.* **2017**, *117*, 5521−5577.

(19) Wang, Y. J.; Szantai-Kis, D. M.; Petersson, E. J. Semi-Synthesis of Thioamide Containing Proteins. *Org. Biomol. Chem.* **2015**, *13*, 5074−5081.

(20) Kloss, F.; Chiriac, A. I.; Hertweck, C. Mapping of the Modular Closthioamide Architecture Reveals Crucial Motifs of Polythioamide Antibiotics. *Chem. - Eur. J.* **2014**, *20*, 15451−15458.

(21) Thee, S.; Garcia-Prats, A. J.; Donald, P. R.; Hesseling, A. C.; Schaaf, H. S. A Review of the Use of Ethionamide and Prothionamide in Childhood Tuberculosis. *Tuberculosis* **2016**, *97*, 126−136.

(22) Dunbar, K. L.; Büttner, H.; Molloy, E. M.; Dell, M.; Kumpfmüller, J.; Hertweck, C. Genome Editing Reveals Novel Thiotemplated Assembly of Polythioamide Antibiotics in Anaerobic Bacteria. *Angew. Chem., Int. Ed.* **2018**, *57*, 14080−14084.

(23) Mahanta, N.; Szantai-Kis, D. M.; Petersson, E. J.; Mitchell, D. A. Biosynthesis and Chemical Applications of Thioamides. *ACS Chem. Biol.* **2019**, *14*, 142−163.
(24) Nauha, E.; Nissinen, M. Co-Crystals of an Agrochemical Active − a Pyridine-Amine Synthon for a Thioamide Group. *J. Mol. Struct.* **2011**, *1006*, 566−569.
(25) Xu, Z.-M.; Li, H.-X.; Young, D. J.; Zhu, D.-L.; Li, H.-Y.; Lang, J.-P. Exogenous Photosensitizer-, Metal-, and Base-Free Visible-Light-Promoted C−H Thiolation Via Reverse Hydrogen Atom Transfer. *Org. Lett.* **2019**, *21*, 237−241.
(26) Crank, G.; Mursyidi, A. Photochemical Reactions of Thioamides. *J. Photochem. Photobiol., A* **1990**, *53*, 301−310.
(27) Hill, J. E.; Linder, M. K.; Davies, K. S.; Sawada, G. A.; Morgan, J.; Ohulchanskyy, T. Y.; Detty, M. R. Selenorhodamine Photosensitizers for Photodynamic Therapy of P-Glycoprotein-Expressing Cancer Cells. *J. Med. Chem.* **2014**, *57*, 8622−8634.
(28) Misra, S. K.; Tewari, U. C. Complexing Behaviour of Aromatic Thioamides (Arcsnhcor). Transition Metal Complexes of N-Carboethoxy-4-Chlorobenzene- and N-Carboethoxy-4-Bromobenzene Thioamide Ligands. *Transition Met. Chem.* **2002**, *27*, 120−125.
(29) Okamoto, K.; Kuwabara, J.; Kanbara, T. Thioamide-Based Transition Metal Complexes. In *Chemistry of Thioamides*; Murai, T., Ed.; Springer: Singapore, 2019; pp 157−191.
(30) Raper, E. S. Copper Complexes of Heterocyclic Thioamides and Related Ligands. *Coord. Chem. Rev.* **1994**, *129*, 91−156.
(31) Ahmad, S.; Hanif, M.; Monim-ul-Mehboob, M.; Isab, A. A.; Alotaibi, M. A.; Ahmad, T. Versatile Coordination Chemistry of Mixed Ligand Silver(I) Complexes of Phosphanes and Thioamides: Structural Features and Biological Properties. *Polyhedron* **2022**, *214*, No. 115643.
(32) Xiong, Z.; Wang, N.; Dai, M.; Li, A.; Chen, J.; Yang, Z. Synthesis of Novel Palladacycles and Their Application in Heck and Suzuki Reactions under Aerobic Conditions. *Org. Lett.* **2004**, *6*, 3337−3340.
(33) Raja, M. U.; Ramesh, R.; Liu, Y. New Binuclear Pd(II) Thioamide Complexes for the Heck Reaction of Aryl Bromides. *Tetrahedron Lett.* **2011**, *52*, 5427−5430.
(34) Sindhuja, E.; Ramesh, R.; Liu, Y. Palladium(II) Thiocarboxamide Complexes: Synthesis, Characterisation and Application to Catalytic Suzuki Coupling Reactions. *Dalton Trans.* **2012**, *41*, 5351−5361.
(35) Sindhuja, E.; Ramesh, R.; Balaji, S.; Liu, Y. Direct Synthesis of Amides from Coupling of Alcohols and Amines Catalyzed by Ruthenium(II) Thiocarboxamide Complexes under Aerobic Conditions. *Organometallics* **2014**, *33*, 4269−4278.
(36) Raja, M. U.; Ramesh, R. Cationic Arene Ruthenium(II) Complexes Bearing N, S Chelating Thiocarboxamides: Synthesis, Structure, Characterization and Catalytic Oxidation of Alcohols. *J. Organomet. Chem.* **2012**, *699*, 5−11.
(37) Tan, P. W.; Mak, A. M.; Sullivan, M. B.; Dixon, D. J.; Seayad, J. Thioamide-Directed Cobalt(III)-Catalyzed Selective Amidation of $C(Sp^3)$−H Bonds. *Angew. Chem., Int. Ed.* **2017**, *56*, 16550−16554.
(38) Mundlapati, V. R.; Gautam, S.; Sahoo, D. K.; Ghosh, A.; Biswal, H. S. Thioamide, a Hydrogen Bond Acceptor in Proteins and Nucleic Acids. *J. Phys. Chem. Lett.* **2017**, *8*, 4573−4579.
(39) Mutoh, Y.; Sakigawara, M.; Niiyama, I.; Saito, S.; Ishii, Y. Synthesis of Rhodium−Primary Thioamide Complexes and Their Desulfurization Leading to Rhodium Sulfido Cubane-Type Clusters and Nitriles. *Organometallics* **2014**, *33*, 5414−5422.
(40) Inamoto, K.; Hasegawa, C.; Hiroya, K.; Doi, T. Palladium-Catalyzed Synthesis of 2-Substituted Benzothiazoles Via a C−H Functionalization/Intramolecular C−S Bond Formation Process. *Org. Lett.* **2008**, *10*, 5147−5150.
(41) Saraiah, B.; Gautam, V.; Acharya, A.; Pasha, M. A.; Hiriyakkanavar, I. One-Pot Synthesis of 2-(Aryl/Alkyl)Amino-3-Cyanobenzo[*b*]Thiophenes and Their Hetero-Fused Analogues by Pd-Catalyzed Intramolecular Oxidative C−H Functionalization/Arylthiolation. *Eur. J. Org. Chem.* **2017**, *37*, 5679−5688.
(42) Jain, P.; Verma, P.; Xia, G.; Yu, J.-Q. Enantioselective Amine A-Functionalization Via Palladium-Catalysed C−H Arylation of Thioamides. *Nat. Chem.* **2017**, *9*, 140−144.
(43) Spangler, J. E.; Kobayashi, Y.; Verma, P.; Wang, D.-H.; Yu, J.-Q. A-Arylation of Saturated Azacycles and N-Methylamines Via Palladium(II)-Catalyzed $C(Sp^3)$−H Coupling. *J. Am. Chem. Soc.* **2015**, *137*, 11876−11879.
(44) Hipler, F.; Gil Girol, S.; Azzam, W.; Fischer, R. A.; Wöll, C. Interaction of Thiadiazole Additives with Metal Surfaces: Reactions and Thin-Film Formation on Gold as a Model Surface. *Langmuir* **2003**, *19*, 6072−6080.
(45) de Freitas Paulo, T.; de Oliveira Pinheiro, S.; Da Silva, M. A. S.; de França Lopes, L. G.; Pinheiro, L. S.; Aquino, G. F. A.; Temperini, M. L. A.; de Lima Neto, P.; Diógenes, I. C. N. Thionicotinamide Sam on Gold: Adsorption Studies and Electroactivity. *Electroanalysis* **2009**, *21*, 1081−1089.
(46) Aoki, H.; Bühlmann, P.; Umezawa, Y. Self-Assembly of a Tricarboxylate Receptor through Thioamide Groups and Its Use for Electrochemical Detection of Protonated Amines. *J. Electroanal. Chem.* **1999**, *473*, 105−112.
(47) Pinheiro, L. S.; Temperini, M. L. A. Coadsorption of 2-Mercaptopyrimidine and 1,10′-Phenanthroline on Au(111) as Seen by Stm. *Surf. Sci.* **1999**, *441*, 53−64.
(48) Pinheiro, L. S.; Temperini, M. L. A. Interaction of 2-Mercaptopyrimidine and 4,4′-Bipyridine and Competition Experiments between Bipyridines and 1,10′-Phenanthroline for the Thiol Layer on Au(111) by Stm. *Appl. Surf. Sci.* **2001**, *171*, 89−100.
(49) Brunetti, V.; Blum, B.; Salvarezza, R. C.; Arvia, A. J.; Schilardi, P. L.; Cuesta, A.; Gayone, J. E.; Zampieri, G. Scanning Tunneling Microscopy, Fourier Transform Infrared Reflection−Absorption Spectroscopy, and X-Ray Photoelectron Spectroscopy of Thiourea Adsorption from Aqueous Solutions on Silver (111). *J. Phys. Chem. B* **2002**, *106*, 9831−9838.
(50) Brunetti, V.; Blum, B.; Salvarezza, R. C.; Arvia, A. J. Comparative Molecular Resolution Stm Imaging of Thiourea, Ethylthiourea, and Sulfur Self-Assembled Adlayer Structures on Silver (111). *Langmuir* **2003**, *19*, 5336−5343.
(51) Mes, T.; Cantekin, S.; Balkenende, D. W. R.; Frissen, M. M. M.; Gillissen, M. A. J.; De Waal, B. F. M.; Voets, I. K.; Meijer, E. W.; Palmans, A. R. A. Thioamides: Versatile Bonds to Induce Directional and Cooperative Hydrogen Bonding in Supramolecular Polymers. *Chem. - Eur. J.* **2013**, *19*, 8642−8649.
(52) Genorio, B.; He, T.; Meden, A.; Polanc, S.; Jamnik, J.; Tour, J. M. Synthesis and Self-Assembly of Thio Derivatives of Calix[4]Arene on Noble Metal Surfaces. *Langmuir* **2008**, *24*, 11523−11532.
(53) Shokri, S. Quinodization Reaction of Naphthalene Diimides to Afford Novel P-Naphthoquinodimethane Light-Harvesting Chromophores: Aromaticity, Photophysics and Application for Photon Upconversion, Ph.D. Thesis; Illinois Institute of Technology: Chicago, 2018.
(54) Shokri, S.; Li, J.; Manna, M. K.; Wiederrecht, G. P.; Gosztola, D. J.; Ugrinov, A.; Jockusch, S.; Rogachev, A. Y.; Ayitou, A. J.-L. A Naphtho-P-Quinodimethane Exhibiting Baird's (Anti)Aromaticity, Broken Symmetry, and Attractive Photoluminescence. *J. Org. Chem.* **2017**, *82*, 10167−10173.
(55) Kamatham, N.; Li, J.; Shokri, S.; Yang, G.; Jockusch, S.; Rogachev, A. Y.; Ayitou, A. J.-L. Quinoidization of Π-Expanded Aromatic Diimides: Photophysics, Aromaticity, and Stability of the Novel Quinoidal Acenes. *Eur. J. Org. Chem.* **2020**, *8*, 917−922.
(56) Shokri, S.; Wiederrecht, G. P.; Gosztola, D. J.; Ayitou, A. J.-L. Photon Upconversion Using Baird-Type (Anti)Aromatic Quinoidal Naphthalene Derivative as a Sensitizer. *J. Phys. Chem. C* **2017**, *121*, 23377−23382.
(57) Yun, Y. J.; Kamatham, N.; Manna, M. K.; Li, J.; Liu, S.; Wiederrecht, G. P.; Gosztola, D. J.; Diroll, B. T.; Rogachev, A. Y.; Ayitou, A. J.-L. Interplay between Energy and Charge Transfers in a Polyaromatic Triplet Donor−Acceptor Dyad. *J. Phy. Chem. C* **2020**, *124*, 12205−12212.

https://doi.org/10.1021/acs.jpcc.3c01663
J. Phys. Chem. C XXXX, XXX, XXX−XXX

(58) Yun, Y. J.; Manna, M. K.; Kamatham, N.; Li, J.; Liu, S.; Peccati, F.; Pemberton, B. C.; Wiederrecht, G. P.; Gosztola, D. J.; Jiménez-Osés, G.; et al. Synthesis and Photophysics of Phenylene Based Triplet Donor−Acceptor Dyads: Ortho Vs. Para Positional Effect on Intramolecular Triplet Energy Transfer. *J. Photochem. Photobiol.* **2022**, *10*, No. 100112.
(59) Yun, Y. J.; Isokuortti, J.; Laaksonen, T.; Durandin, N.; Ayitou, A. J.-L. Triplet-Triplet Annihilation Photon-Upconversion in Hydrophilic Media with Biorelevant Cholesteryl Triplet Energy Acceptors. *J. Photochem. Photobiol., A* **2021**, *418*, No. 113412.
(60) Maharjan, S.; Yun, Y. J.; Okello, V. A.; Wiederrecht, G. P.; Gosztola, D. J.; Ayitou, A. J.-L. Photometric Sensing of Heavy Metal Ions Using a Naphthoquinodimethyl-Bis-Thioamide Dye: Selectivity & Photophysics of the Metal Organic Complexes. *J. Photochem. Photobiol., A* **2022**, *424*, No. 113648.
(61) Mahapatra, S.; Li, L.; Schultz, J. F.; Jiang, N. Methods to Fabricate and Recycle Plasmonic Probes for Ultrahigh Vacuum Scanning Tunneling Microscopy-Based Tip-Enhanced Raman Spectroscopy. *J. Raman Spectrosc.* **2021**, *52*, 573−580.
(62) Horcas, I.; Fernández, R.; Gómez-Rodríguez, J. M.; Colchero, J.; Gómez-Herrero, J.; Baro, A. M. Wsxm: A Software for Scanning Probe Microscopy and a Tool for Nanotechnology. *Rev. Sci. Instrum.* **2007**, *78*, No. 013705.
(63) Kresse, G.; Furthmüller, J. Efficient Iterative Schemes for Ab Initio Total-Energy Calculations Using a Plane-Wave Basis Set. *Phys. Rev. B* **1996**, *54*, 11169−11186.
(64) Blöchl, P. E. Projector Augmented-Wave Method. *Phys. Rev. B* **1994**, *50*, 17953−17979.
(65) Perdew, J. P.; Burke, K.; Ernzerhof, M. Generalized Gradient Approximation Made Simple. *Phys. Rev. Lett.* **1996**, *77*, 3865−3868.
(66) Klimeš, J.; Bowler, D. R.; Michaelides, A. Van Der Waals Density Functionals Applied to Solids. *Phys. Rev. B* **2011**, *83*, No. 195131.
(67) Dion, M.; Rydberg, H.; Schröder, E.; Langreth, D. C.; Lundqvist, B. I. Van Der Waals Density Functional for General Geometries. *Phys. Rev. Lett.* **2004**, *92*, No. 246401.
(68) Vericat, C.; Vela, M. E.; Benitez, G.; Carro, P.; Salvarezza, R. C. Self-Assembled Monolayers of Thiols and Dithiols on Gold: New Challenges for a Well-Known System. *Chem. Soc. Rev.* **2010**, *39*, 1805−1834.
(69) Engel, S.; Fritz, E.-C.; Ravoo, B. J. New Trends in the Functionalization of Metallic Gold: From Organosulfur Ligands to N-Heterocyclic Carbenes. *Chem. Soc. Rev.* **2017**, *46*, 2057−2075.
(70) Häkkinen, H. The Gold−Sulfur Interface at the Nanoscale. *Nat. Chem.* **2012**, *4*, 443−455.
(71) Daniel, M.-C.; Astruc, D. Gold Nanoparticles: Assembly, Supramolecular Chemistry, Quantum-Size-Related Properties, and Applications toward Biology, Catalysis, and Nanotechnology. *Chem. Rev.* **2004**, *104*, 293−346.
(72) Meyer, J. A.; Baikie, I. D.; Kopatzki, E.; Behm, R. J. Preferential Island Nucleation at the Elbows of the Au(111) Herringbone Reconstruction through Place Exchange. *Surf. Sci.* **1996**, *365*, L647−L651.
(73) Narasimhan, S.; Vanderbilt, D. Elastic Stress Domains and the Herringbone Reconstruction on Au(111). *Phys. Rev. Lett.* **1992**, *69*, 1564−1567.
(74) Hanke, F.; Björk, J. Structure and Local Reactivity of the Au(111) Surface Reconstruction. *Phys. Rev. B* **2013**, *87*, No. 235422.
(75) Bartelt, N. C.; Thürmer, K. Structure and Energetics of the Elbows in the Au(111) Herringbone Reconstruction. *Phys. Rev. B* **2021**, *104*, No. 165425.
(76) Jiang, N.; Zhang, Y. Y.; Liu, Q.; Cheng, Z. H.; Deng, Z. T.; Du, S. X.; Gao, H. J.; Beck, M. J.; Pantelides, S. T. Diffusivity Control in Molecule-on-Metal Systems Using Electric Fields. *Nano Lett.* **2010**, *10*, 1184−1188.
(77) Écija, D.; Otero, R.; Sánchez, L.; Gallego, J. M.; Wang, Y.; Alcamí, M.; Martín, F.; Martín, N.; Miranda, R. Crossover Site-Selectivity in the Adsorption of the Fullerene Derivative Pcbm on Au(111). *Angew. Chem., Int. Ed.* **2007**, *46*, 7874−7877.
(78) Vranik, R.; Stetsovych, V.; Feigl, S.; Müllegger, S. Stable Π-Radical 2,2-Diphenyl-1-Picrylhydrazyl (Dpph) Adsorbed at the Elbows of 22×3 Reconstructed Au(111). *Surf. Sci.* **2020**, *700*, No. 121676.
(79) Cheng, Z. H.; Gao, L.; Deng, Z. T.; Liu, Q.; Jiang, N.; Lin, X.; He, X. B.; Du, S. X.; Gao, H. J. Epitaxial Growth of Iron Phthalocyanine at the Initial Stage on Au(111) Surface. *J. Phy. Chem. C* **2007**, *111*, 2656−2660.
(80) Dubois, L. H.; Zegarski, B. R.; Nuzzo, R. G. Molecular Ordering of Organosulfur Compounds on Au(111) and Au(100): Adsorption from Solution and in Ultrahigh Vacuum. *J. Chem. Phys.* **1993**, *98*, 678−688.
(81) Pan, S.; Yang, P.; Zhu, L.; Hong, M.; Xie, C.; Zhou, F.; Shi, Y.; Huan, Y.; Cui, F.; Zhang, Y. Effect of Substrate Symmetry on the Orientations of MoS_2 Monolayers. *Nanotechnology* **2021**, *32*, No. 095601.
(82) Van Hove, M. A.; Koestner, R. J.; Stair, P. C.; Bibérian, J. P.; Kesmodel, L. L.; BartoŠ, I.; Somorjai, G. A. The Surface Reconstructions of the (100) Crystal Faces of Iridium, Platinum and Gold: I. Experimental Observations and Possible Structural Models. *Surf. Sci.* **1981**, *103*, 189−217.
(83) Binnig, O. K.; Rohrer, H.; Gerber, C.; Stoll, E. Real-Space Observation of the Reconstruction of Au(100). *Surf. Sci.* **1984**, *144*, 321−335.
(84) Ercolessi, F.; Tosatti, E.; Parrinello, M. Au (100) Surface Reconstruction. *Phys. Rev. Lett.* **1986**, *57*, 719−722.
(85) Gao, X.; Hamelin, A.; Weaver, M. J. Potential-Dependent Reconstruction at Ordered Au(100)-Aqueous Interfaces as Probed by Atomic-Resolution Scanning Tunneling Microscopy. *Phys. Rev. Lett.* **1991**, *67*, 618−621.
(86) Trembułowicz, A.; Sabik, A.; Grodzicki, M. Au(100) as a Template for Pentacene Monolayer. *Molecules* **2021**, *26*, No. 2393.
(87) Spurgeon, P. M.; Liu, D.-J.; Walen, H.; Oh, J.; Yang, H. J.; Kim, Y.; Thiel, P. A. Characteristics of Sulfur Atoms Adsorbed on Ag(100), Ag(110), and Ag(111) as Probed with Scanning Tunneling Microscopy: Experiment and Theory. *Phys. Chem. Chem. Phys.* **2019**, *21*, 10540−10551.
(88) Shen, M.; Russell, S. M.; Liu, D.-J.; Thiel, P. A. Destabilization of Ag Nanoislands on Ag(100) by Adsorbed Sulfur. *J. Chem. Phys.* **2011**, *135*, No. 154701.
(89) Russell, S. M.; Shen, M.; Liu, D.-J.; Thiel, P. A. Adsorption of Sulfur on Ag(100). *Surf. Sci.* **2011**, *605*, 520−527.
(90) Chae, M. Y.; Czarnik, A. W. Fluorometric Chemodosimetry. Mercury(II) and Silver(I) Indication in Water Via Enhanced Fluorescence Signaling. *J. Am. Chem. Soc.* **1992**, *114*, 9704−9705.
(91) Tsukamoto, K.; Shinohara, Y.; Iwasaki, S.; Maeda, H. A Coumarin-Based Fluorescent Probe for Hg^{2+} and Ag^{+} with an N′-Acetylthioureido Group as a Fluorescence Switch. *Chem. Commun.* **2011**, *47*, 5073−5075.
(92) Hwang, K. S.; Park, K. Y.; Kim, D. B.; Chang, S.-K. Fluorescence Sensing of Ag^{+} Ions by Desulfurization of an Acetylthiourea Derivative of 2-(2-Hydroxyphenyl)Benzothiazole. *Dyes Pigm.* **2017**, *147*, 413−419.

https://doi.org/10.1021/acs.jpcc.3c01663
J. Phys. Chem. C XXXX, XXX, XXX−XXX